

## Oxidase-mimicking activity of ultrathin MnO<sub>2</sub> nanosheets in a colorimetric assay of chlorothalonil in food samples

Enze Sheng<sup>a,1</sup>, Yuxiao Lu<sup>a,1</sup>, Yuting Tan<sup>b</sup>, Yue Xiao<sup>a</sup>, Zhenxi Li<sup>a</sup>, Zhihui Dai<sup>a,\*</sup>

<sup>a</sup> Jiangsu Collaborative Innovation Center of Biomedical Functional Materials and Jiangsu Key Laboratory of Biofunctional Materials, School of Chemistry and Materials Science, Nanjing Normal University, Nanjing 210023, PR China

<sup>b</sup> Department of Pesticide Science, College of Plant Protection, Nanjing Agricultural University, Nanjing 210095, PR China

### ARTICLE INFO

#### Keywords:

Chlorothalonil  
MnO<sub>2</sub> nanosheets  
Colorimetric assay  
Oxidase-mimicking  
Food samples analysis

### ABSTRACT

Chlorothalonil is a class of 2B carcinogen which is widely used in the prevention and treatment of fungal diseases in food samples. Its residual problem has been increasingly concerned by society. In this paper, a fast and simple colorimetric assay based on Manganese dioxide nanosheets (MnO<sub>2</sub> NSs)-oxidize 3,3',5,5'-tetramethylbenzidine (TMB) platform was used to detect residual pesticide chlorothalonil in food samples. Under optimal conditions, the half maximal inhibitory concentration and the limit of detection of chlorothalonil were 3.27 and 0.024 ng/mL. There were no obvious cross-reactivity between chlorothalonil and interference substances. The recoveries shown the satisfactory results. The results of colorimetric assay for the authentic samples were largely consistent with gas chromatography. Therefore, the proposed method would be convenient and satisfactory analytical methods for the monitoring of chlorothalonil. Furthermore, the MnO<sub>2</sub> – TMB system was used to produce test strips for quick and convenient visual detection of chlorothalonil with good performance.

### 1. Introduction

Recently people pay more and more attention to their own health, and the requirements for food quality are becoming higher and higher (Najafi, Khalilzadeh, & Karimi-maleh, 2014). The analytical methods used to analyze and detect the content of different substances in food have gradually attracted people's attention, and more and more detection methods have been developed by researchers (Baghizadeh & Karimi-maleh, 2015; Eren, Atar, Lütfi, & Karimi-maleh, 2015; Shamsadin, Mohammad, Somaye, & Maleh, 2019). Pesticides widely used to ensure crop yields have also attracted people's attention because of their residual problems.

Chlorothalonil is a kind of non-systemic fungicide developed by the Diamond Alkali (Fermenta) company (Van Scoy & Tjeerdema, 2014). As the world's second most produced fungicide, it is widely used in the cultivation of fruits and vegetables (Simões et al., 2019). Chlorothalonil has significant toxicity, and it is highly toxic to fish and aquatic invertebrates (Guerreiro, Rola, Rovani, Costa, & Sandrini, 2017). It was found that chlorothalonil had a significant carcinogenic effect on the kidneys of rats and had mutagenic effects on their offspring (Guerreiro et al., 2017). Therefore, on October 27, 2017, the World Health Organization, an international Agency for Research on Cancer, listed

chlorothalonil as a class 2B carcinogen. So, it is necessary to establish a rapid, sensitive and economical detection method to detect residual chlorothalonil.

In recent years, many strategies detection of chlorothalonil residues have been explored, including chromatographic analysis, chemiluminescence, enzyme-linked immunosorbent assay, and fluorescence methods (Catalá-Icardo, Gómez-Benito, Simó-Alfonso, & Herrero-Martínez, 2017; dos Santos et al., 2019; Hirakawa et al., 2015; Hou, Zhao, & Liu, 2016; Kurz et al., 2008; Yuan, Wang, Cheng, Kong, & Che, 2019; Sheng, Du, Yang, Hua, & Wang, 2018). However, the traditional methods still exist some disadvantages, such as low detection sensitivity, complex and long operation time and many of them require expensive instruments (Bettencourt Da Silva, Dias, & Camões, 2012; Drabova et al., 2019; López-Blanco et al., 2018; Yang et al., 2018). These insufficiencies clearly limit the wide application of these methods. Therefore, it was necessary to establish new methods with high sensitivity and quantitatively detect the residue of chlorothalonil to meet the increasing needs of food monitoring. Due to its environmental friendliness, inherent simplicity, and high sensitivity, new materials based on biosensing strategies have been paid attention to the field detections design (Yan, Li, Zheng, & Su, 2015). The analysis method based on 3,3',5,5'-tetramethylbenzidine (TMB) can be used to

\* Corresponding author.

E-mail address: [daizhihui@nynu.edu.cn](mailto:daizhihui@nynu.edu.cn) (Z. Dai).

<sup>1</sup> The two authors contribute equally to this article.

quantify analytes quickly and easily without complicated instruments and expensive biological reagents (Hizir et al., 2016; Yan et al., 2018). Manganese oxide nanosheets (MnO<sub>2</sub> NSs) is a nanomaterial with peroxidase-like enzyme activity, which has good biocompatibility (Yan et al., 2017). It can be reduced to Mn<sup>2+</sup> by TMB, and can oxidize large numbers of reducing substrates, providing a promising opportunity for the advanced development of colorimetric assays. It avoids any oxidants (H<sub>2</sub>O<sub>2</sub>) participating in the TMB-based reaction, making handling easier and less time consuming (Yan et al., 2016). Therefore, MnO<sub>2</sub>-TMB-based strategies can be used as promising platform in chemical/biosensing applications (Peng et al., 2019).

Until now, there are few reports about MnO<sub>2</sub>-catalyzed analysis methods for pesticide residues. In this research, a simple and quick colorimetric analysis method for detecting the chlorothalonil residues in food samples was designed. This method not only improved the qualitative and quantitative of the colorimetric sensor but also provided a new design of an enzyme sensor. TMB (colorless) can be oxidized by MnO<sub>2</sub> NSs to oxTMB (blue), which had a characteristic absorption peak at 653 nm. 3-phosphoglyceraldehyde (PGAL) can reduce MnO<sub>2</sub> NSs to generate Mn<sup>2+</sup>, then TMB cannot be oxidized. Under phosphoric acid conditions, PGAL can be decomposed by glyceraldehyde-3-phosphate dehydrogenase (GAPD) and coenzyme I (NAD), so that MnO<sub>2</sub> NSs cannot be decomposed and TMB can be oxidized. After the addition of chlorothalonil, as an active inhibitor of GAPD, chlorothalonil can decompose GAPD. Without GAPD, PGAL can oxidize the MnO<sub>2</sub> NSs. Therefore, the sensor platform can show an obvious color change when the concentration of the added chlorothalonil had been changed. What is more, the sensor platform could be made into a test strip of paper to quickly and visually detect the residue of chlorothalonil during on-site testing.

## 2. Materials and methods

### 2.1. Materials and instruments

The standards of chlorothalonil (99.3%) and its interfering substances were supplied by the Jiangsu Pesticide Research Institute (Jiangsu, China). NAD, KMnO<sub>4</sub>, TMB, PGAL, 4-morpholineethane sulfonic acid (SDBS), GAPD, bovine serum albumin (BSA), and other analytical chemicals were obtained from Sigma-Aldrich Corporation. The transmission electron microscopy (TEM) images were obtained on a JEOL-2100F apparatus (Japan). X-ray photoelectron spectra (XPS) were obtained using a scanning X-ray microprobe (PHI 5000 Versa, ULACPHI, Inc. Japan). A Cary 60 UV-Vis spectrometer (Agilent, USA) was used to carry out UV-Vis absorbance measurements. The Fourier transform infrared spectroscopy (FTIR) images were obtained on a Lambda 950 (USA). The colorimetric assay was validated with an Agilent 7890A gas chromatography (GC) (Agilent, USA).

### 2.2. Preparation of MnO<sub>2</sub> NSs

Ultrathin MnO<sub>2</sub> NSs were prepared as previous described with some modifications (Kai et al., 2012). In brief, 3.2 mL SDBS (0.5 mol/L), 0.16 mL H<sub>2</sub>SO<sub>4</sub> solution (0.1 mol/L), 6.4 mL ethanol and 48 mL distilled water were mixed together and the mixture was stirred at 90 °C for 15 min. 0.64 mL of KMnO<sub>4</sub> solution (0.05 mol/L) was added into the solution and stirred for 60 min. Deionization water was used for washing three times to purify the synthesized MnO<sub>2</sub> NSs. Finally, for further use, the MnO<sub>2</sub> NSs were freeze-dried forming a brownish black powder.

### 2.3. Assays for PGAL activity

50 μL PGAL, 20 μL MnO<sub>2</sub> NSs (0.5 mg/mL), 25 μL TMB (1 mg/mL) and 100 μL NaAc were mixed together, diluted to 500 μL by PB buffer (10 mmol/L) and incubated at 37 °C for 15 min. The conjugates were

verified by UV-vis spectroscopy at 653 nm for analysis.

### 2.4. Preparation for chlorothalonil sensing

When GAPD and NAD were added, PGAL could be catalytically hydrolyzed to produce diphosphoglycerate, which could not initiate the decomposition of MnO<sub>2</sub> NSs. Due to action of chlorothalonil, the GAPD was decomposed, preventing the decomposition of PGAL and causing the decrease of absorbance. Different concentrations (25 μL) of chlorothalonil and GAPD were mixed at 37 °C for 30 min. Then NAD and PAGL in PB buffer were added at 37 °C. Next, 20 μL MnO<sub>2</sub> NSs, 25 μL TMB solution, and 100 μL NaAc buffer were added. Finally, the mixed solution was diluted to 500 μL with ultrapure water. After incubating at 37 °C for 15 min, the UV-vis spectra were detected.

The mean values of Inhibition Efficiency (IE) were calculated: IE

$$= (A_{\text{inhibitor}} - A_{\text{no inhibitor}}) / (A_0 - A_{\text{no inhibitor}}) \times 100\%$$

A<sub>inhibitor</sub>: the absorbance of MnO<sub>2</sub>-TMB/PGAL/GAPD with chlorothalonil.

A<sub>no inhibitor</sub>: the absorbance of MnO<sub>2</sub>-TMB/PGAL/GAPD without chlorothalonil.

A<sub>0</sub>: the absorbance of MnO<sub>2</sub>-TMB.

The inhibitory concentration (IC<sub>50</sub> and IC<sub>10</sub>) were obtained from a four-parameter logistic equation of the sigmoidal curves using Origin Pro 8.0 software (Sheng et al., 2016).

### 2.5. Assay optimization

As an important component of the sensor, GAPD reduced the sensitivity of the sensor if its concentration was too high, while a low concentration could cause a high system background. At the same time, the catalytic activity of GAPD was related to many conditions, such as pH, reaction temperature, and incubation time. In order to improve the sensitivity of the system to detect chlorothalonil, the parameters of the system were optimized.

### 2.6. Gas chromatographic analysis and validation

20 g of sample (wheat, rice, apple, pear, grape, tomato, cucumber and cabbage), 10 mL of water and 60 mL of acetonitrile were mixed together and shaken for 1 h. Then the organic phase was dehydrated and concentrated, the samples were diluted with 2 mL of acetone and further analyzed by GC-ECD (Bettencourt Da Silva et al., 2012). A DB-1 fused silica capillary column (30 m × 0.32 mm × 0.25 μm) was used for the detection. The column temperature was initially held at 150 °C in 2 min, then raised to 210 °C by 6 °C/min, and finally raised to 270 °C by 30 °C/min, and held at this value for 6 min. Nitrogen was used as the carrier gas (58 mL/min). The detector was an ECD at a temperature of 320 °C. The measured results were compared with the colorimetric assay.

## 3. Results and discussion

### 3.1. The characterization of MnO<sub>2</sub> NSs

In this study, the ultrathin MnO<sub>2</sub> NSs were characterized by TEM, XPS, FTIR and UV-Vis spectroscopy. A large two-dimensional structure with an average transverse size of nearly 50 nm (Fig. 1A), indicated the nanostructures provided a large surface area for the reaction with TMB. The UV-Vis spectra of MnO<sub>2</sub> NSs are 300–600 nm, and the characteristic absorption was near the 380 nm (Fig. 1B). In the FTIR spectrum, 3423 cm<sup>-1</sup> was corresponded to O–H stretching modes of interlayer water molecules and H-bonded O–H groups attributed to bending mode of water molecules was observed near 1629 cm<sup>-1</sup>. The absorption peak at 1116 cm<sup>-1</sup> was attributed to the O–H bending vibration

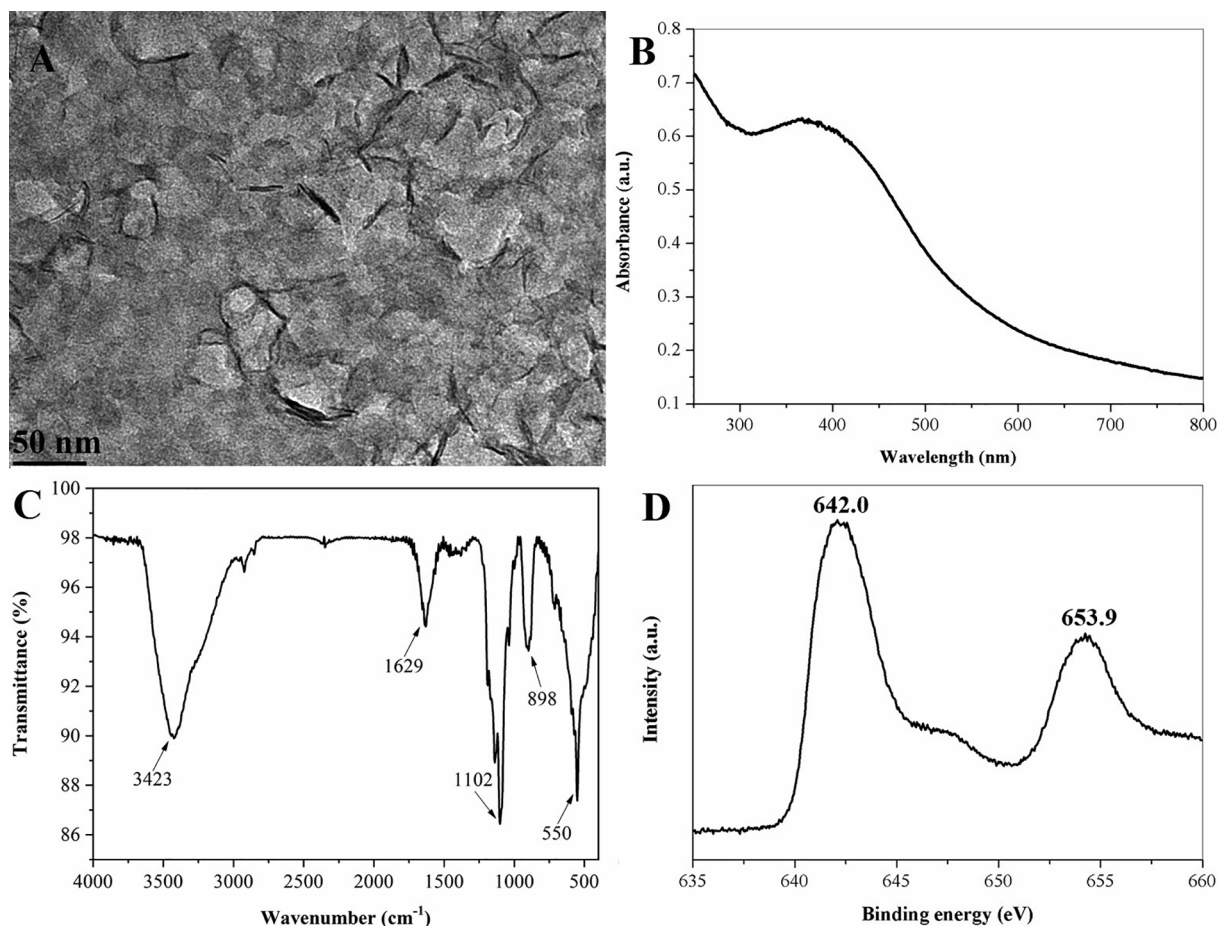


**Fig. 1.** (A) The TEM images, (B) the UV-vis absorption spectra of MnO<sub>2</sub> NSs, (C) The FTIR spectra of MnO<sub>2</sub> NSs, (D) The XPS spectra of MnO<sub>2</sub> NSs.

combined with Mn atoms. The peaks at 898 and 550 cm<sup>-1</sup> were the main characteristic absorption bands corresponding to stretching vibration of the MnO<sub>2</sub>, 550–900 cm<sup>-1</sup> to the M-O, M-O-M and O-M-O lattice vibrations (Fig. 1C). The XPS of the MnO<sub>2</sub> NSs exhibited two peaks centered at 642.0 eV and 653.9 eV, belonging to Mn<sub>2p3/2</sub> and Mn<sub>2p1/2</sub> (Fig. 1D). All of the results demonstrate the successful preparation of ultrathin MnO<sub>2</sub> NSs.

### 3.2. The catalytic performance of MnO<sub>2</sub> NSs

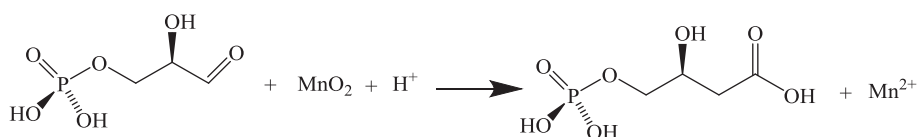
The colorimetric assay established in this study was based on the color changing reaction of MnO<sub>2</sub>-TMB as a signal output. Therefore, the catalytic capacity of the MnO<sub>2</sub> NSs was the key to construct colorimetric analysis. To verify the catalytic performance, MnO<sub>2</sub> NSs were directly incubated with TMB to catalyze the colorimetric reactions. The TMB solution had no obvious absorption peak (Fig. 2A, curve b) within the range of 330–800 nm, while MnO<sub>2</sub> NSs had an absorption peak at 380 nm (Fig. 2A, curve a). When MnO<sub>2</sub> NSs and TMB were mixed, two strong characteristic peaks appeared at 371 nm and 653 nm (Fig. 2A, curve c) respectively, which corresponded to oxTMB, and the solution turned blue (inset photograph in Fig. 2A). This indicated that the MnO<sub>2</sub>

NSs had oxidase-like activity.

In order to value the oxidase-like properties of MnO<sub>2</sub> NSs, different concentrations of MnO<sub>2</sub> NSs were incubated with TMB and the absorption values of each system were measured. The results are shown in Fig. 2B. With the concentration of MnO<sub>2</sub> NSs increased, the absorbance at 653 nm increased correspondingly, and the amount of oxTMB also increased. At the same time, the color of the mixed solution changed from colorless to dark blue (Fig. 2C). Therefore, the enzyme simulation activity of MnO<sub>2</sub> NSs changed the absorbance of the solution. Stability was an important thing to evaluate the performance of the test methods. The stability of the system was studied for more than 30 min (Fig. 2D). The absorbance intensity kept unchanged, without obvious changes at 653 nm, which indicated that the MnO<sub>2</sub>-TMB system had good consistency performance and could be used to manufacture sensor platforms.

### 3.3. Feasibility verification of enzyme controlled MnO<sub>2</sub>-TMB platform

MnO<sub>2</sub> NSs could oxidize TMB (colorless) to produce oxTMB (blue) (Fig. 3A, curve a). In the presence of PGAL, PGAL could induce cleavage of the MnO<sub>2</sub> NSs and prevent oxidation of TMB (Fig. 3A, curve b).



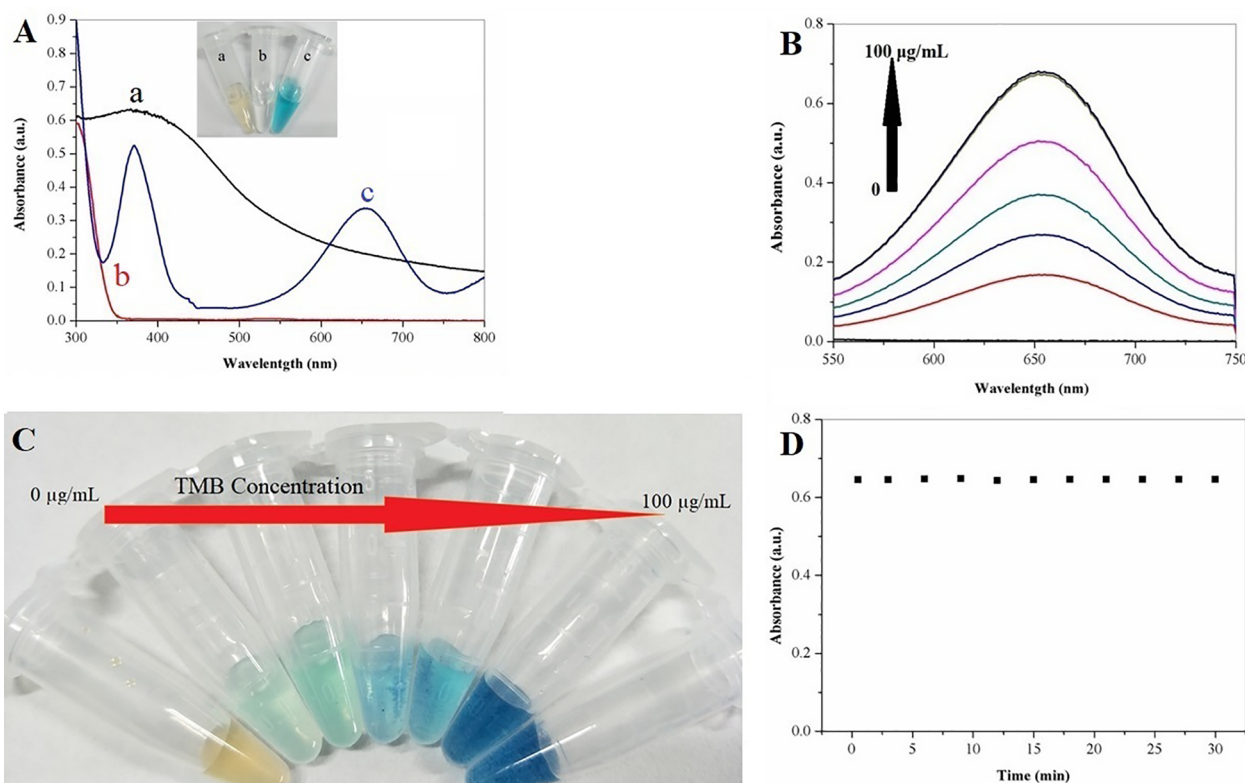


**Fig. 2.** (A) The UV-vis absorption spectra of  $\text{MnO}_2$  NSs (a), TMB (b), and  $\text{MnO}_2$  NSs + TMB (c). (B) The UV-vis absorption spectra of TMB with different concentrations of  $\text{MnO}_2$  NSs. (C) The corresponding photographs of the probe solution taken under daylight. (D) The stability of the  $\text{MnO}_2$ -TMB system was systematically investigated with 30 min.

PGAL itself has an aldehyde group and will be oxidized to produce phosphoglycerate (Wang & Alaupovic, 1980). The interaction between  $\text{MnO}_2$  NSs and PGAL were verified by UV-vis spectroscopy. As shown in Fig. 3B, the curve a showed the UV absorption of  $\text{MnO}_2$  NSs, after the addition of PGAL into the system, the characteristic peak of the  $\text{MnO}_2$  NSs at 380 nm was reduced (Fig. 3B, curve b), indicating that PGAL could decompose the  $\text{MnO}_2$  NSs and prevent the oxidation of TMB. When GAPD was introduced into the system, GAPD reacted with PGAL to form 1,3-bisphosphoglyceric acid preferentially, which prevented the cleavage of PGAL and  $\text{MnO}_2$  NSs, leading to the oxidation of TMB at 653 nm (Fig. 3A, curve c) (Dunham et al., 1983). However, after the addition of chlorothalonil, the chlorothalonil inhibited the activity of GAPD and the enzyme activity was inhibited so that the decomposition reaction of PGAL and the  $\text{MnO}_2$  NSs was not prevented, thus reducing the absorption peak. Therefore, a simple and economical method was produced for the analysis of chlorothalonil.

In order to evaluate the feasibility of this method, the absorbance intensity of the  $\text{MnO}_2$ -TMB (curve a), GAPD- $\text{MnO}_2$ -TMB (curve b), CHL- $\text{MnO}_2$ -TMB (curve c), and CHL-GAPD-PGAL- $\text{MnO}_2$ -TMB (curve d) systems were analyzed (Fig. 3C). The absorbance was not affected by GAPD (50  $\mu\text{g/mL}$ ) or chlorothalonil (10  $\mu\text{g/mL}$ ) alone at 653 nm (curve b and curve c were nearly same with curve a). When 50  $\mu\text{g/mL}$  GAPD and 10  $\mu\text{g/mL}$  chlorothalonil were present in the system, the absorbance intensity decreased by nearly 73% (curve d). Furthermore, the effects of  $\text{Mn}^{2+}$  (the decomposition product of  $\text{MnO}_2$  NSs) on the TMB solution were tested. No absorption peak was observed, and the color of the solution did not change regardless of whether  $\text{Mn}^{2+}$  was added (Fig. 3D). In view of the results, a colorimetric assay for laboratory detection of chlorothalonil was established by the oxidation reaction of TMB catalyzed by  $\text{MnO}_2$  NSs.

### 3.4. Optimization

The effect of pH on the system in the presence of 10 mU/mL GAPD was studied, and the results are shown in Fig. S1A. The absorbance ratio was obviously enhanced as the pH value increased from 4.5 to 6.5, and then an apparent decrease in the absorbance ratio was observed in the pH range of 7.5–9.5. These results showed that the hydrolysis efficiency of GAPD had good performance in an acidic medium. As shown in Fig. S1B, the absorbance ratio continuously increased with the increasing temperature and reached a maximum at 37 °C. The enzymatic reactions were consecutively monitored by UV-vis 5 min after adding different concentrations of GAPD (5, 10 and 20  $\mu\text{g/mL}$ ) at 37 °C (Fig. S1C). The absorbance intensity at an enzymolysis time point of 30 min was plotted as a function of the GAPD activity. Due to the above results, we chose pH 6.5 PB buffer as the optimal buffer, 37 °C as the reaction temperature, and 30 min as the proper reaction time for hydrolyzing PGAL by GAPD.

As shown in Fig. S1D, with the increase of GAPD concentration (0–50 mU/mL), the absorbance at 653 nm decreased continuously, and the color changed from colorless to blue (Fig. S1E). The absorbance of the system under different concentrations of GAPD was shown in Fig. S1D. There is a good linear relationship between the absorbance ratio of the system and the concentration of GAPD. Finally, 20 mU/mL GAPD was chosen for the assay to detect chlorothalonil.

### 3.5. Sensitivities

Under the optimal reaction conditions, the standard curves of chlorothalonil were obtained by the colorimetric assay (Fig. 4). The assay was shown to have an  $\text{IC}_{50}$  of 3.27 ng/mL, the  $\text{IC}_{10}$ - $\text{IC}_{90}$  was 0.45–3430 ng/mL. More importantly, the sensor could directly detect chlorothalonil down to 0.45 ng/mL, which was much lower than the maximum residue limit (MRL) (0.01 mg/kg in USA) (Lin et al., 2019).

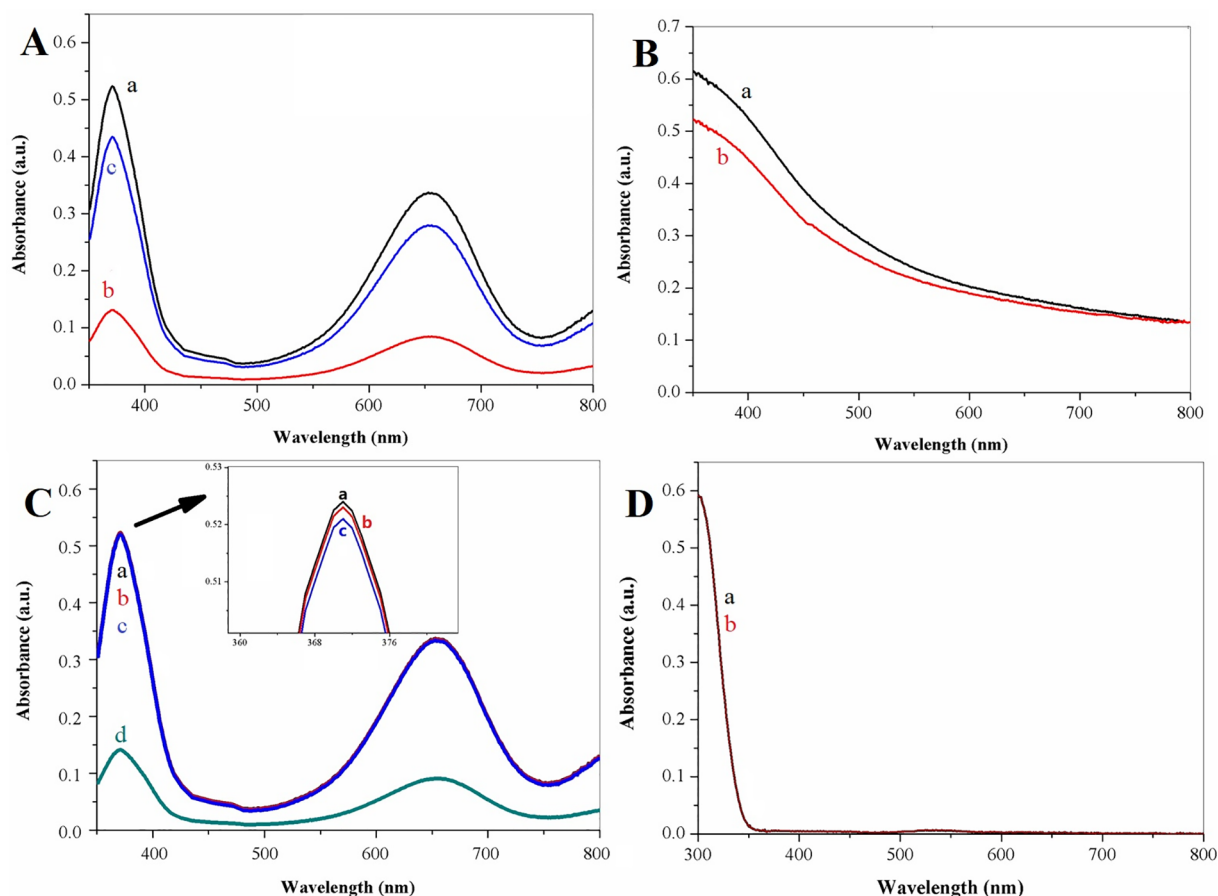


**Fig. 3.** (A) The UV-vis absorption spectra of  $\text{MnO}_2$  + TMB (a),  $\text{MnO}_2$  + TMB + PGAL (b), and  $\text{MnO}_2$  + TMB + PGAL + GAPD (c). (B) The UV-vis absorption spectra of  $\text{MnO}_2$  NSs in the absence (a) and presence (b) of PGAL. (C) The UV-vis absorption spectra of  $\text{MnO}_2$  + TMB (a),  $\text{MnO}_2$  + TMB + GAPD (b), and  $\text{MnO}_2$  + TMB + PGAL + GAPD + chlorothalonil (c). (D) UV-vis absorption spectra of the TMB system in the absence (a) and presence (b) of  $\text{Mn}^{2+}$ .

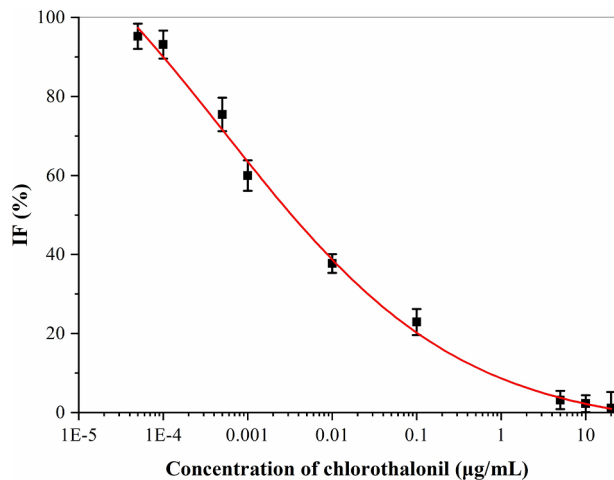


**Fig. 4.** Standard inhibition curves for chlorothalonil using colorimetric assay by the  $\text{MnO}_2$  NSs.

The lowest detectable concentration (LOD) for chlorothalonil was 0.024 ng/mL, which was much lower than the existing reporting methods (Table S1). Therefore, the system meets the requirements for detecting chlorothalonil residues.

### 3.6. Detection of chlorothalonil, using test strips

In order to meet the requirements of rapid detection of pesticide

residues, a paper-based sensor was constructed for chlorothalonil. The  $\text{MnO}_2$  NSs were dispersed in ultrapure water, then sprayed on a qualitative filter paper and stored in the dark for 30 d. When “TYT” was written on the paper with TMB as ink, the blue color was immediately displayed on the test paper and the color remained unchanged for 30 min (Fig. 5A). Then, 50  $\mu\text{L}$  of the mixed buffer (containing PGAL, GAPD, TMB, and chlorothalonil (standard solution)) was dripped onto one prepared piece of test paper. The color of the test paper was visually observed as the concentration of chlorothalonil increased (X) (Fig. 5B). The assay was shown to have a testing range from 0.001 to 0.5  $\mu\text{g}/\text{mL}$ , which was much lower than the MRL. These results showed that the paper-based sensor was capable of visually indicating the residue of different concentrations of chlorothalonil. This method was simple, reliable, easy to operate, and fast in response.

### 3.7. Analytical figure of merit

In order to evaluate the specificity of the detection method, we tested the blank different varieties food samples and food samples added with the same concentration of chlorothalonil. As shown in Fig. S2A, the results of the blank food samples were almost the same, and the results of food samples with chlorothalonil were also similar. This indicated that these common interference substances could not significantly interfere with chlorothalonil detection. In the use of chlorothalonil, it was usually mixed with some other pesticides. We selected some common pesticides to evaluate the accuracy of the method. Although these interfering substances were often used in combination with chlorothalonil, but their bacteriostatic mechanism were different from chlorothalonil and hardly reacts with PGAL and GAPD. The results

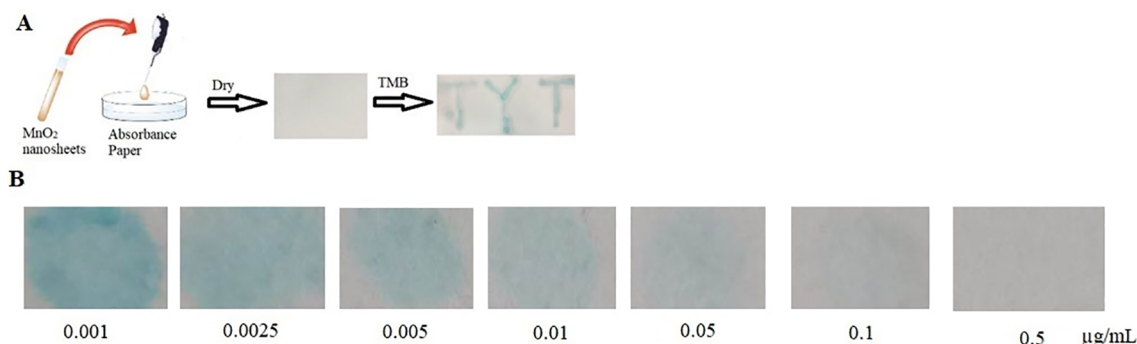


**Fig. 5.** (A) Demonstrating the feasibility of test strips by handwriting on the paper using TMB solution as ink. (B)  $\text{MnO}_2$  NSs-based test strips for visual detection of chlorothalonil. The concentrations of chlorothalonil were 0.001, 0.0025, 0.005, 0.01, 0.05, 0.1, 0.5  $\mu\text{g/mL}$ .

**Table 1**  
The recoveries of samples spiked with Chlorothalonil by colorimetric assay.

Sample	Chlorothalonil		
	Spiked concentration (ng/g)	Found concentration (ng/g)	Mean recovery $\pm$ SD (% , n = 3)
Wheat	10	9.27	92.7 $\pm$ 2.98
	100	91.52	91.5 $\pm$ 3.45
	1000	853.41	85.3 $\pm$ 5.49
Rice	10	9.35	93.5 $\pm$ 3.69
	100	86.29	86.3 $\pm$ 5.82
	1000	1002.21	100.2 $\pm$ 3.23
Apple	10	9.61	96.1 $\pm$ 3.69
	100	99.21	99.2 $\pm$ 5.62
	1000	952.87	95.3 $\pm$ 2.87
Pear	10	9.21	92.1 $\pm$ 4.69
	100	103.15	100.3 $\pm$ 3.74
	1000	875.34	87.5 $\pm$ 3.96
Grape	10	9.84	98.4 $\pm$ 7.43
	100	94.66	94.7 $\pm$ 3.65
	1000	1005.36	100.5 $\pm$ 5.78
Tomato	10	10.28	102.8 $\pm$ 4.52
	100	98.37	98.4 $\pm$ 4.36
	1000	1024.78	102.4 $\pm$ 3.56
Cucumber	10	8.97	89.7 $\pm$ 8.82
	100	94.28	94.3 $\pm$ 5.89
	1000	934.49	93.4 $\pm$ 3.47
Cabbage	10	8.88	88.8 $\pm$ 5.27
	100	93.63	93.6 $\pm$ 3.21
	1000	908.41	90.8 $\pm$ 2.82

showed that the pesticides often used in combination with CHL could not significantly interfere with  $\text{MnO}_2$ -TMB (Fig. S2B). Combined with the results, it indicated that our biosensor had a good specificity in detecting chlorothalonil.

The dilution was used to minimize matrix effects (Fig. S2). The recoveries of method were 85.3%–102.8% and the relative standard deviations (RSDs) were 2.82–8.82% (Table 1). The results met the requirements of quantitative detection, which was according to the guidelines on the pesticide residue trials of China (NY/T 788-2018). These results indicated that the colorimetric assays were accurate and reliable to determine if chlorothalonil was present in food samples.

The results of correlation between the colorimetric assay and GC for analyses of samples with chlorothalonil (Table S2). Good correlations were obtained between GC and colorimetric assays ( $y = 0.9953x + 2.0337$ ,  $R^2 = 0.9965$ ) (Fig. S4). These results suggested that the colorimetric assays were reliable for quantitative detection of chlorothalonil in food samples.

#### 4. Conclusions

A novel and sensitive colorimetric assay was developed successfully.

The  $\text{MnO}_2$  NSs prepared in this study were simple to prepare, have a wide absorption range (300–600 nm), and were able to imitate oxidase properties well. The  $\text{MnO}_2$  NSs catalytic reaction does not require the participation of  $\text{H}_2\text{O}_2$ , making detection simpler. Under the optimal detection conditions, the linear range for chlorothalonil was 0.45–3430 ng/mL and LOD was 0.024 ng/mL. Compared with traditional detection methods and other detection methods, this colorimetric assay has higher sensitivity, wider linear range, good stability, good selectivity and shorter detection time. In addition, the  $\text{MnO}_2$ -TMB platform has been successfully established for manufacture paper-based device for detecting chlorothalonil with qualitative and quantitative. The two assays were implemented to measure chlorothalonil in food samples with satisfactory results and good repeatability.

#### CRedit authorship contribution statement

**Enze Sheng:** Conceptualization, Methodology, Formal analysis, Visualization, Software, Writing - original draft. **Yuxiao Lu:** Validation, Formal analysis, Visualization, Software. **Yuting Tan:** Validation, Formal analysis, Visualization, Software. **Yue Xiao:** Formal analysis. **Zhenxi Li:** Formal analysis. **Zhihui Dai:** Conceptualization, Methodology, Resources, Writing - original draft, Writing - review & editing, Supervision, Project administration, Funding acquisition.

#### Declaration of Competing Interest

The authors declare that they have no known competing financial interests or personal relationships that could have appeared to influence the work reported in this paper.

#### Acknowledgement

This work was supported by the Natural Science Foundation of China for the project (Nos. 21625502 and 21974070).

#### Appendix A. Supplementary data

Supplementary data to this article can be found online at <https://doi.org/10.1016/j.foodchem.2020.127090>.

#### References

- Baghizadeh, A., & Karimi-maleh, H. (2015). A Voltammetric Sensor for Simultaneous Determination of Vitamin C and Vitamin B 6 in Food Samples Using  $\text{ZrO}_2$  Nanoparticle/Ionic Liquids Carbon Paste Electrode. 549–557.
- Bettencourt Da Silva, R. J. N., Dias, P. M. V. B. F., & Camões, M. F. G. F. C. (2012). Development and validation of a grouping method for pesticides analysed in food-stuffs. *Food Chemistry*, 134(4), 2291–2302.
- Catalá-Icardo, M., Gómez-Benito, C., Simó-Alfonso, E. F., & Herrero-Martínez, J. M. (2017). Determination of azoxystrobin and chlorothalonil using a methacrylate-based polymer modified with gold nanoparticles as solid-phase extraction sorbent.

- Analytical and Bioanalytical Chemistry*, 409(1), 243–250.
- dos Santos, E. O., Gonzales, J. O., Ores, J. C., Marube, L. C., Caldas, S. S., Furlong, E. B., & Primel, E. G. (2019). Sand as a Solid support in ultrasound-assisted MSPD: A simple, green and low-cost method for multiresidue pesticide determination in fruits and vegetables. *Food Chemistry*, 297(February), Article 124926.
- Drabova, L., Alvarez-Rivera, G., Suchanova, M., Schusterova, D., Pulkrabova, J., Tomaniova, M., ... Hajslova, J. (2019). Food fraud in oegano: Pesticide residues as adulteration markers. *Food Chemistry*, 276(June 2018), 726–734.
- Dunham, J., Dodds, R., Nahir, A., Frost, G., Catterall, A., Bitensky, L., & Chayen, J. (1983). Aerobic glycolysis of bone and cartilage: The possible involvement of fatty acid oxidation. *Cell Biochemistry and Function*, 1, 168–172.
- Eren, T., Atar, N., Lütfi, M., & Karimi-maleh, H. (2015). A sensitive molecularly imprinted polymer based quartz crystal microbalance nanosensor for selective determination of lovastatin in red yeast rice. *Food Chemistry*, 185, 430–436.
- da Guerreiro, A. S., Rola, R. C., Rovani, M. T., da Costa, S. R., & Sandrini, J. Z. (2017). Antifouling biocides: Impairment of bivalve immune system by chlorothalonil. *Aquatic Toxicology*, 189(April), 194–199.
- Hirakawa, Y., Yamasaki, T., Watanabe, E., Okazaki, F., Murakami-Yamaguchi, Y., Oda, M., ... Miyake, S. (2015). Development of an immunosensor for determination of the fungicide chlorothalonil in vegetables, using surface plasmon resonance. *Journal of Agricultural and Food Chemistry*, 63(28), 6325–6330.
- Hizir, M. S., Top, M., Balcioglu, M., Rana, M., Robertson, N. M., Shen, F., ... Yigit, M. V. (2016). Multiplexed activity of peroxidase: DNA-capped AuNPs act as adjustable peroxidase. *Analytical Chemistry*, 88(1), 600–605.
- Hou, F., Zhao, L., & Liu, F. (2016). Determination of chlorothalonil residue in cabbage by a modified QuEChERS-based extraction and gas chromatography-mass spectrometry. *Food Analytical Methods*, 9(3), 656–663.
- Kai, K., Kobayashi, Y., Yamada, Y., Miyazaki, K., Abe, T., Uchimoto, Y., & Kageyama, H. (2012). Electrochemical characterization of single-layer MnO<sub>2</sub> nanosheets as a high-capacitance pseudocapacitor electrode. *Journal of Materials Chemistry*, 22(29), 14691–14695.
- Kurz, M. H. S., Gonçalves, F. F., Adaime, M. B., Da Costa, I. F. D., Primel, E. G., & Zanella, R. (2008). A gas chromatographic method for the determination of the fungicide chlorothalonil in tomatoes and cucumbers and its application to dissipation studies in experimental greenhouses. *Journal of the Brazilian Chemical Society*, 19(6), 1129–1135.
- Lin, H., Zhao, S., Fan, X., Ma, Y., Wu, X., Su, Y., & Hu, J. (2019). Residue behavior and dietary risk assessment of chlorothalonil and its metabolite SDS-3701 in water spinach to propose maximum residue limit (MRL). *Regulatory Toxicology and Pharmacology*, 107(June), Article 104416.
- López-Blanco, R., Moreno-González, D., Nortes-Méndez, R., García-Reyes, J. F., Molina-Díaz, A., & Gilbert-López, B. (2018). Experimental and theoretical determination of pesticide processing factors to model their behavior during virgin olive oil production. *Food Chemistry*, 239, 9–16.
- Najafi, M., Khalilzadeh, M. A., & Karimi-maleh, H. (2014). A new strategy for determination of bisphenol a in the presence of sudan I using a ZnO / CNTs / ionic liquid paste electrode in food samples. *Food Chemistry*, 158, 125–131.
- Peng, C., Xing, H., Fan, X., Xue, Y., Li, J., & Wang, E. (2019). Glutathione regulated inner filter effect of MnO<sub>2</sub> nanosheets on boron nitride quantum dots for sensitive assay [research-article]. *Analytical Chemistry*, 91(9), 5762–5767.
- Scay, A. R. Van, & Tjeerdema, R. S. (2014). Reviews of Environmental Contamination and Toxicology Volume 232. 232.
- Shamsadin, Z., Mohammad, A., Somaye, A. T., & Maleh, H. K. (2019). A Nanostructure voltammetric platform amplified with ionic liquid for determination of tert-butylhydroxyanisole in the presence kojic acid. *Journal of Food Measurement and Characterization*, 13(3), 1781–1787.
- Sheng, E., Du, M., Yang, J., Hua, X., & Wang, M. (2018). Development of immunoassays for detecting oxyfluorfen residue in agricultural and environmental samples. *RSC Advances*, 8(9), 5020–5025.
- Sheng, E., Shi, H., Zhou, L., Hua, X., Feng, L., Yu, T., & Wang, M. (2016). Dual-labeled time-resolved fluoroimmunoassay for simultaneous detection of clothianidin and diniconazole in agricultural samples. *Food Chemistry*, 192, 525–530.
- Simões, T., Novais, S. C., Natal-da-Luz, T., Leston, S., Rosa, J., Ramos, F., ... Lemos, M. F. L. (2019). Fate and effects of two pesticide formulations in the invertebrate *folsonia candida* using a natural agricultural soil. *Science of the Total Environment*, 675, 90–97.
- Wang, C., & Alaupovic, P. (1980). Glycerinaldehyde-3-phosphate dehydrogenase from human erythrocyte membranes. Kinetic mechanism and competitive substrate inhibition by glyceraldehyde 3-phosphate. *Archives of Biochemistry and Biophysics*, 205(1), 136–145.
- Yan, X., Li, H., Zheng, W., & Su, X. (2015). Visual and fluorescent detection of tyrosinase activity by using a dual-emission ratiometric fluorescence probe. *Analytical Chemistry*, 87(17), 8904–8909.
- Yan, X., Song, Y., Wu, X., Zhu, C., Su, X., Du, D., & Lin, Y. (2017). Oxidase-mimicking activity of ultrathin MnO<sub>2</sub> nanosheets in colorimetric assay of acetylcholinesterase activity. *Nanoscale*, 9(6), 2317–2323.
- Yan, X., Song, Y., Zhu, C., Li, H., Du, D., Su, X., & Lin, Y. (2018). MnO<sub>2</sub> nanosheet-carbon dots sensing platform for sensitive detection of organophosphorus pesticides. *Analytical Chemistry*, 90(4), 2618–2624.
- Yan, X., Song, Y., Zhu, C., Song, J., Du, D., Su, X., & Lin, Y. (2016). Graphene quantum dot-MnO<sub>2</sub> nanosheet based optical sensing platform: A sensitive fluorescence “turn Off-On” nanosensor for glutathione detection and intracellular imaging. *ACS Applied Materials and Interfaces*, 8(34), 21990–21996.
- Yang, M., Gu, Y., Wu, X., Xi, X., Yang, X., Zhou, W., ... Li, J. (2018). Rapid analysis of fungicides in tea infusions using ionic liquid immobilized fabric phase sorptive extraction with the assistance of surfactant fungicides analysis using IL-FPSE assisted with surfactant. *Food Chemistry*, 239, 797–805.
- Yuan, Y. Y., Wang, S. T., Cheng, Q., Kong, D. M., & Che, X. G. (2019). Simultaneous determination of carbendazim and chlorothalonil pesticide residues in peanut oil using excitation-emission matrix fluorescence coupled with three-way calibration method. *Spectrochimica Acta – Part A: Molecular and Biomolecular Spectroscopy*, 220, Article 117088.